Pharm Res (2017) 34:1716–1727
DOI 10.1007/s11095-017-2180-9

RESEARCH PAPER

Systematic Investigation of the Role of Surfactant Composition and Choice of oil: Design of a Nanoemulsion-Based Adjuvant Inducing Concomitant Humoral and CD4$^+$ T-Cell Responses

Signe Tandrup Schmidt[1,2] • Malene Aaby Neustrup[1] • Stine Harloff-Helleberg[1] • Karen Smith Korsholm[2] • Thomas Rades[1] • Peter Andersen[2] • Dennis Christensen[2] • Camilla Foged[1]

Received: 11 November 2016 / Accepted: 11 May 2017 / Published online: 17 May 2017

ABSTRACT

Purpose Induction of cell-mediated immune (CMI) responses is crucial for vaccine-mediated protection against difficult vaccine targets, e.g., *Chlamydia trachomatis (Ct)*. Adjuvants are included in subunit vaccines to potentiate immune responses, but many marketed adjuvants stimulate predominantly humoral immune responses. Therefore, there is an unmet medical need for new adjuvants, which potentiate humoral and CMI responses. The purpose was to design an oil-in-water nanoemulsion adjuvant containing a synthetic CMI-inducing mycobacterial monomycoloyl glycerol (MMG) analogue to concomitantly induce humoral and CMI responses.

Methods The influence of emulsion composition was analyzed using a systematic approach. Three factors were varied: i) saturation of the oil phase, ii) type and saturation of the applied surfactant mixture, and iii) surfactant mixture net charge.

Results The emulsions were colloidally stable with a droplet diameter of 150–250 nm, and the zeta-potential correlated closely with the net charge of the surfactant mixture. Only cationic emulsions containing the unsaturated surfactant mixture induced concomitant humoral and CMI responses upon immunization of mice with a *Ct* antigen, and the responses were enhanced when squalene was applied as the oil phase. In contrast, emulsions with neutral and net negative zeta-potentials did not induce CMI responses. The saturation degree of the oil phase did not influence the adjuvanticity.

Conclusion Cationic, MMG analogue-containing nanoemulsions are potential adjuvants for vaccines against pathogens for which both humoral and CMI responses are needed.

KEY WORDS adjuvant · drug delivery · emulsion · immune response · vaccine

ABBREVIATIONS

CAF	Cationic adjuvant formulation
CMI	Cell-mediated immunity
Cryo-TEM	Cryo-transmission electron microscopy
Ct	*Chlamydia trachomatis*
DDA	Dimethyldioctadecylammonium bromide
DODAC	Dioleoyldimethylammonium chloride
DOPE	Dioleoylphosphoethanolamine
DSPE	Distearoylphosphoethanolamine
GLA	Glucopyranosyl lipid A
GRAS	Generally regarded as safe
HA	Hemagglutinin
HEPES	4-(2-hydroxyethyl)-1-piperazineethanesulfonic acid
HLB	Hydrophile-lipophile balance
HRP	Horseradish peroxidase
HSM	High shear mixing
IFN	Interferon
IL	Interleukin
LN	Lymph node
MHC	Major histocompatibility complex
MMG-1	Monomycoloyl glycerol
MOMP	Major outer membrane protein
Mtb	*Mycobacterium tuberculosis*
o/w	Oil-in-water
PDI	Polydispersity index

Dennis Christensen and Camilla Foged shared senior authorship.

Electronic supplementary material The online version of this article (doi:10.1007/s11095-017-2180-9) contains supplementary material, which is available to authorized users.

✉ Camilla Foged
camilla.foged@sund.ku.dk

[1] Department of Pharmacy, Faculty of Health and Medical Sciences, University of Copenhagen, Universitetsparken 2, 2100 Copenhagen Ø, Denmark

[2] Statens Serum Institut, Department of Infectious Disease Immunology, Artillerivej 5, 2300 Copenhagen S, Denmark

PMA	Phorbol-12-myristate-13-acetate
Pos:neu	Positive-to-neutral
RSV	Respiratory syncytial virus
rt.	Room temperature
S.c.	Subcutaneous
TDB	Trehalose-6,6′-dibehenate
TIV	Trivalent influenza vaccine
TMB	3,3′,5,5′-tetramethylbenzidine
Tris	Tris(hydroxymethyl)aminomethane
w/o	Water-in-oil
z-average	Intensity-weighted average hydrodynamic diameter

INTRODUCTION

Vaccination is generally considered as the most cost-effective medical invention ever, and it has contributed to a remarkable increase in the public health at a level comparable to what has been achieved by providing general access to clean water and good hygiene (1). However, there are still a number of challenges that must be overcome in future vaccine development strategies (2). One example is that licensed vaccines are mainly efficacious against pathogens, where infection can be prevented with an antibody response (1). In contrast, it is more challenging to design efficacious vaccines against pathogens, where prevention of infection also requires the stimulation of T-cell responses, e.g., *Chlamydia trachomatis* (*Ct*) and influenza virus (1,3). The pathogen-specific antigens in subunit vaccines often possess low intrinsic immunogenicity, providing the need for inclusion of adjuvants, which can be specifically tailored to induce T-cell and/or humoral responses. New adjuvants, which are capable of concomitantly inducing strong humoral and T-cell responses, may therefore potentially fulfill the immunological requirements for future vaccines against such difficult pathogens.

Immunopotentiators, which can stimulate and/or modulate immune responses, have been widely used in combination with liposome-based delivery systems. Examples are the cationic adjuvant formulations (CAFs, Statens Serum Institut, Copenhagen, DK) in which cationic dimethyldioctadecylammonium (DDA) bromide is combined with an immunostimulator, e.g., trehalose-6,6′-dibehenate (TDB, CAF01), or a synthetic analogue of monomycoloyl glycerol (MMG-1), respectively (4–7). Liposomes comprised of DDA and MMG-1 (CAF04) have been shown to induce strong antigen-specific $CD4^+$ T-cell responses, when administered subcutaneously (s.c.), but the humoral responses they induce are relatively weak (7). We therefore hypothesized that appropriate incorporation of DDA and MMG-1 into an emulsion inducing strong humoral responses might enable the design of an adjuvant capable of stimulating concomitant cell-mediated immune (CMI) responses.

Emulsions have been extensively evaluated as adjuvants for subunit vaccines in combination with peptide and protein antigens. A number of oil-in-water (o/w) emulsions based on squalene are approved for clinical use [MF59 and AS03 (GlaxoSmithKline, UK)], or are clinically tested [AF03 (Sanofi Pasteur, Lyon, FR) and glucopyranosyl lipid A-stable emulsion (GLA-SE, Infectious Diseases Research Institute, Seattle, WA, USA)] (8). These emulsions are generally reported to stimulate strong antibody responses in the clinic (9,10). For example, monovalent, inactivated H7N9 influenza virus adjuvanted with AS03 or MF59 were shown to significantly increase the geometric mean antibody titer towards hemagglutinin (HA) in adults compared to the unadjuvanted virus vaccine (9). Likewise, a trivalent influenza vaccine (TIV) adjuvanted with MF59 induced significantly stronger antibody responses in infants aged 6–72 months compared to the unadjuvanted TIV and a split vaccine (10). However, more recent data suggest that an emulsion adjuvant in combination with an immunopotentiator induces stronger CMI responses than the emulsion adjuvant alone (11).

Emulsions consist of an immiscible oil phase dispersed in a continuous water phase (o/w), or vice versa for water-in-oil (w/o) emulsions. Stabilization of the interface can be achieved by incorporation of surfactant(s) resulting in reduced surface tension on the dispersed droplets (12). A number of different surfactants are generally regarded as safe (GRAS) and used in clinically approved emulsions, e.g., certain types of polysorbates (Tween) and sorbitans (Span). The MF59 emulsion thus contains Tween 80 and Span 85 (8).

In the present study, we investigated the influence of the type of oil and the type of surfactant mixture (surfactant + amphiphilic immunopotentiator, referred to as S_{mix}, Tables I and II) on the physicochemical properties and the capability of MMG-1-containing emulsions to induce concomitant $CD4^+$ T-cell and humoral responses. Therefore, S_{mix} with systematically varied physicochemical properties were designed (Table II) and emulsified with unsaturated squalene or saturated squalane as the oil phase and Tris-buffer as the water phase. The S_{mix} contained either unsaturated (Tween 80, Span 80) or saturated (Tween 60, Span 60) surfactants, respectively. The surface charge was varied systematically by incorporating either unsaturated or saturated lipid with a cationic headgroup [dioleoyldimethylammonium chloride (DODAC) or DDA, respectively], an unsaturated or a saturated lipid with a zwitterionic headgroup [dioleoylphosphoethanolamine (DOPE) or distearoylphosphoethanolamine

Table I Experimentally Tested Formulation Variables. The Pos:neu Lipid Molar Ratio is Defined as the Molar Ratio of DDA:DSPE, or DODA:DOPE, in the Emulsions, Respectively

	Factor		
Type of oil	Squalene	Squalane	
Type of S_{mix}	Unsaturated	Saturated	
Pos:neu lipid molar ratio	2:0	1:1	0:2

Table II The Composition of the Surfactant Mixtures (referred to as S_{mix} no. 1–6). The Amount of Each Component in Each Mixture is Given as Dose (μg/dose) in a Dose volume of 100 μl with 10 mg Squalene or Squalane. In the Saturated S_{mix} (no. 1–3), Span and Tween 60, MMG, DDA and DSPE were Used, Whereas the Unsaturated S_{mix} (no. 4–6) Contained Span and Tween 80, MMG, DODA and DOPE

S_{mix} no.	1	2	3	4	5	6
	Saturated			Unsaturated		
Span	960					
Tween	1040					
MMG	100					
Pos. lipid	200	100	0	185	92	0
Neu. lipid	0	119	237	0	118	236
Pos:neu lipid molar ratio	2:0	1:1	0:2	2:0	1:1	0:2

(DSPE), respectively], or a 1:1 M mixture of cationic and zwitterionic unsaturated or saturated lipid (Table I). The emulsification process was optimized towards achieving i) monodisperse emulsion droplet size distributions below 250 nm in average hydrodynamic diameter, and ii) colloidally stable emulsions. The capability of the emulsions to induce humoral and $CD4^+$ T-cell responses was compared to the responses induced with CAF04.

We show that the recombinant vaccine candidate *Ct* major outer membrane protein (MOMP)-based fusion antigen CTH522 (13), adjuvanted with emulsions containing MMG-1 and displaying a net positive surface charge, is capable of inducing antigen-specific humoral responses at higher levels than the levels measured for CAF04, while the CMI responses are comparable. Furthermore, we demonstrate that vaccines based on emulsions containing the unsaturated, net positive S_{mix} induce stronger CMI responses compared to vaccines based on emulsions containing the saturated, net positive S_{mix}.

MATERIALS AND METHODS

Materials

Squalene, squalane, Tween 60 + 80 and Span 60 + 80 were obtained from Sigma-Aldrich (St. Louis, MO, USA). DDA and MMG-1 (7) were purchased from Clausson Kaas (Farum, DK), DSPE and DOPE were acquired from Avanti Polar Lipids (Alabaster, AL, USA), and DODAC was obtained from Northern Lipids (Burnaby, BC, CA). All other chemicals were used at analytical grade and purchased from commercial suppliers.

Preparation of Emulsions

Weighed amounts of Span 80, MMG-1, DDA, DSPE, DODAC, and DOPE, respectively, were dissolved in 99% (*v*/v) EtOH and mixed in glass vials resulting in the surfactant mixtures specified in Table II. The mixtures were dried under a gentle N_2 stream for 2 h followed by air-drying overnight to remove trace amounts of EtOH. Span 60 was weighed into the appropriate dry surfactant mixtures, as it is poorly soluble in EtOH. The oil phase was weighed into the vials and heated at 60°C for 10 min with intermittent mixing to melt the surfactants and the oil phase. The water phase consisted of Tween 60 or 80 dissolved in tris(hydroxymethyl)aminomethane (Tris)-buffer (10 mM, pH 7.4), and it was added to the oil phase after melting. A pre-emulsion was prepared by high shear mixing (HSM) by using a Heidolph Silent Crusher equipped with a 6F shearing tool (Heidolph Instruments GmbH, Schwabach, DE) at 60°C and 26,000 rpm for 5 min, which was subsequently microfluidized by using a LV1 Low Volume Homogenizer (Microfluidics, Westwood, MA, USA) with six passes at 20,000 psi. The final emulsions were sterile-filtered through a 0.22 μm filter (Sartorius Stedim Biotech GmbH, Goettingen, DE) prior to vaccination.

Preparation of CAF04

Weighed amounts of DDA and MMG-1 were dissolved in 99% (*v*/v) EtOH and mixed in a glass vial at a molar ratio of 82:18. The lipid mixture was dried under a gentle N_2 stream for 2 h followed by air-drying overnight to remove trace amounts of EtOH. The lipid film was rehydrated in Tris-buffer by HSM for 15 min as described above. The final lipid concentration in the resulting dispersion was 2.5/0.5 mg/ml DDA/MMG.

Ternary Phase Diagram

Construction of a ternary phase diagram of formulations containing squalene and saturated S_{mix} with DDA was performed by pre-mixing squalene and S_{mix} at different molar ratios (1:9, 2:8 and so forth) with subsequent titration in Tris-buffer (Fig. 1). Each mixture was emulsified by HSM as described above at 60°C and 26,000 rpm for 5 min. The resulting mixtures were analyzed with light microscopy and polarized light microscopy by using an Axiolab E microscope (Carl Zeiss Microscopy GmbH, Jena, DE) and analyzed with Motic Images Plus 2.0 software (Motic, Hong Kong, CN). The mixtures were identified as o/w or w/o emulsions, respectively, and the presence of S_{mix} crystals was noted.

Physicochemical Characterization

The intensity-weighted average hydrodynamic diameter (*z*-average) and polydispersity index (PDI) of the emulsion were determined by dynamic light scattering (DLS) using the photon correlation spectroscopy technique. Undiluted samples were analyzed at 25°C using a Zetasizer Nano ZS (Malvern

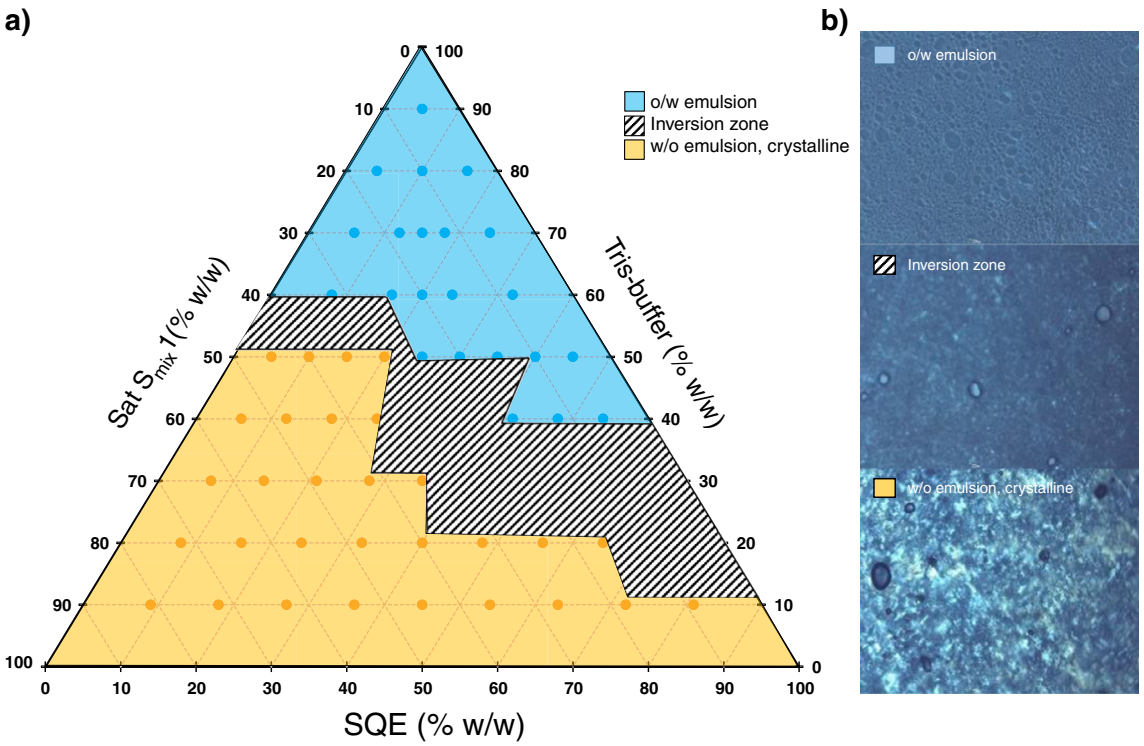

Fig. 1 **(a)** Mixtures prepared at different ratios (% *w/w*) of squalene and Sat $S_{mix}1$ were titrated with Tris-buffer, and a ternary phase diagram was constructed. Yellow: w/o emulsion region, possibly with crystalline structures. Blue: o/w emulsion region. Hatched area: Inversion zone. The w/o emulsions contained crystals of S_{mix} components that could not be dissolved in the oil phase, and the amount of crystals correlated with the ratio of S_{mix}. **(b)** Representative polarized light microscopy images of ternary mixtures. Top: o/w emulsion 25% (*w/w*) squalene, 25% (*w/w*) Sat $S_{mix}1$, 50% (*w/w*) Tris-buffer. Middle: inversion zone 30% (*w/w*) squalene, 30% (*w/w*) Sat $S_{mix}1$, 40% (*w/w*) Tris-buffer. Bottom: w/o emulsion w crystalline structures 45% (*w/w*) squalene, 45% (*w/w*) Sat $S_{mix}1$, 10% (*w/w*) Tris-buffer.

Instruments Ltd., Worcestershire, UK) equipped with a 633 nm laser and 173° detection optics. The measurements were not affected by the sample concentration within the range used in the present study. For viscosity and refractive indexes, the values of Tris-buffer were used. The particle size distribution was reflected in the PDI, which ranges from 0 for a monodisperse to 1.0 for an entirely heterodisperse dispersion. Laser-Doppler electrophoresis was used to determine the zeta-potential of the emulsions diluted 100 times in MilliQ-water. Zetasizer Software version 7.11 (Malvern Instruments Ltd) was used for acquisition and analysis of the data. The morphology of the emulsions was investigated by cryo-transmission electron microscopy (cryo-TEM) using a Tecnai G2 20 TWIN transmission electron microscope (FEI, Hillsboro, OR, USA) mounted with a 4x4 K charged-coupled device Eagle camera from FEI, essentially as described elsewhere (5). The emulsions prepared at a positive-to-neutral (pos:neu) lipid molar ratio of 2:0 were further evaluated by small deformation rheology using an AR-G2 Rheometer (TA Instruments-Waters LLC, New Castle, DE, USA) equipped with a cone-Peltier plate geometry (diameter of 40 mm and a 1° cone angle) and a solvent trap system. The emulsions were vortexed for 15 s prior to the measurements to ensure sample homogeneity. A sample volume of 0.30 mL was used, which was mounted directly on the lower geometry kept at 23.0 ± 0.1°C. A conditioning step was performed with pre-shear at shear stress of 0.05 Pa for 10 s followed by 5 min equilibration time, followed by a frequency sweep with an increasing angular frequency from 0.01 to 100.0 rad/s. Four points were collected per decade and the oscillation stress was set to 0.015 Pa. Before running the stress sweep, a second conditioning step was conducted. The sweeps were performed for each emulsion, where the oscillation stress was increased from 0.001 to 10 Pa at a step size of six to eight points per decade with a constant frequency of 0.100 Hz.

Immunization of Mice

All animal experiments were conducted in accordance with the national Danish guidelines for animal experiments as approved by the Danish Council for Animal Experiments and in accordance with EU directive 2010/63/EU. All procedures were refined to provide maximal comfort and minimal stress for the animals. Female, 6–8 week old C57BL/6 mice were purchased from Harlan (Horst, NL) and allowed free access to food and water. Groups of four mice were immunized twice with three-week intervals s.c. at the base of the tail with a dose volume of 100 µl and 5 µg CTH522 (54 kD, provided by Department of Vaccine Development, Statens Serum Institut), which was mixed with the adjuvants 30 min prior to administration (13). The dose

of the emulsions is given in Table II. Unadjuvanted CTH522 was used as the negative control, and CTH522 adjuvanted with CAF04 (250/50 μg DDA/MMG-1 in 100 μl pr. dose) was used as the positive control, respectively.

Preparation of Organs

Immune responses were evaluated two weeks after the final immunization. The spleens and the draining, inguinal lymph nodes (LNs) were harvested, and the blood was collected. Serum was isolated from the blood by centrifugation at 10,000 g for 10 min. Single cell suspensions were obtained from the spleen and LNs by passing the organs through a nylon mesh cell-strainer followed by washing with phosphate-buffered saline (PBS) and RPMI 1640 (Gibco Invitrogen, Carlsbad, CA, USA). The cells were resuspended in RPMI 1640 supplemented with 10% (*v*/v) heat-inactivated fetal bovine serum, $5x10^{-6}$ M β-mercaptoethanol, 1% (*v*/v) penicillin-streptomycin, 1% (*v*/v) sodium pyruvate, 1 mM L-glutamine, and 10 mM 4-(2-hydroxyethyl)-1-piperazineethanesulfonic acid (HEPES), as described elsewhere (7).

Quantification of Interferon (IFN)-γ

Single-cell suspensions of splenocytes were restimulated in 96 well-plates containing $2x10^5$ cells/well for 4 days at 37°C with 5 μg CTH522, while Concavalin A (5 μg/ml, Sigma-Aldrich) or medium alone served as positive and negative controls, respectively. The IFN-γ concentration in the supernatant was measured by using an enzyme-linked immunosorbent assay (ELISA) kit (BD Biosciences, San Jose, CA, USA), as described previously (7). Briefly, MaxiSorp plates (Nunc, Roskilde, DK) were coated with capture anti-mouse IFN-γ antibody overnight at 4°C. Following blocking with 2% (*w*/*v*) skim-milk powder dispersed in PBS, the supernatants were added to the wells at eight-fold dilution in PBS. After 2 h incubation at room temperature (rt), biotin anti-IFN-γ was added, followed by streptavidin-conjugated horseradish peroxidase (HRP). Detection was performed with 3,3′,5,5′-tetramethylbenzidine (TMB, Kem-En-Tec, Taastrup, DK), and the reaction was stopped with 0.2 M H_2SO_4. The optical density was read at 450 nm with 570 nm correction.

Intracellular Flow Cytometry Analysis

The percentage of antigen-specific cytokine-producing $CD4^+$ T cells relative to the total population of $CD4^+$ T cells in response to restimulation with the antigen was determined by using intracellular flow cytometry. Briefly, isolated splenocytes or lymphocytes (10^6 cells/well) were stimulated for 6 h at 37°C with either 5 μg/well CTH522, supplemented RPMI 1640 medium or a phorbol-12-myristate-13-acetate (PMA) and ionomycin mix (both from Sigma-Aldrich), in the presence of anti-mouse CD28 antibody (37.51), anti-mouse CD49d antibody (MFR4.B, both from BD Biosciences) and Brefeldin A (Sigma-Aldrich). The intracellular cytokine staining procedure was performed essentially as described elsewhere (5). The cells were surface-stained with FITC-labelled anti-mouse CD44 antibody (IM7) and eFluor780-conjugated anti-mouse CD4 antibody (RM4–5), and stained intracellularly with APC-labelled anti-mouse IL2 antibody (JES6-5H4), PerCP-Cy5.5-labelled anti-mouse IL17a antibody (eBio17B7), PE-labelled anti-mouse TNF-α antibody (MP6-XT22), and PE-Cy7-labelled anti-mouse IFN-γ antibody (XMG1.2), all from eBiosciences (San Diego, CA, USA). Briefly, cell fixation and permeabilization were done by using BD Cytofix/Cytoperm™ (BD, San Diego, CA, USA) followed by intracellular cytokine staining (Supplementary data, fig. 1). The cells were acquired by flow cytometry using a BD Canto flow cytometer (BD Biosciences), and analyzed by using FlowJo vX software (Tree Star, Ashland, OR, USA).

Measurement of Antibody Levels in Serum

Antigen-specific IgG1 and IgG2c antibody levels in serum were measured by ELISA. MaxiSorp plates were coated with 2 μg/well CTH522 overnight at 4°C. The plates were blocked with 2% (*w*/*v*) bovine serum albumin (Sigma Aldrich) in PBS, and the serum was added in serial dilutions, in a concentration range covering both the maximum and minimum plateau levels, respectively, depending on the isotype. After 2 h incubation at rt., antigen-specific IgG1 and IgG2c were detected with HRP-conjugated rabbit anti-mouse IgG1 antibody (diluted 1:20,000), or HRP-conjugated rabbit anti-mouse IgG2c antibody (diluted 1:5000), respectively. TMB was used as substrate, and the reaction was stopped with 0.2 M H_2SO_4. The optical density was read at 450 nm with 570 nm correction. Antibody endpoint titers were calculated using the method proposed by Frey *et al.*, utilizing the mean and standard deviation of the naïve group to calculate the cut-off at each dilution (14).

Statistical Analysis

One-way ANOVA was used to analyze the difference between the individual groups in GraphPad Prism version 6.05 for Windows (GraphPad Software, La Jolla, CA, USA).

RESULTS

A Systematic Investigation of Emulsion Formulation Parameters

We systematically evaluated the effects of composition on the physicochemical properties (*z*-average, PDI and zeta-

potential) and adjuvanticity of the emulsions. The selected variables included i) saturation of the oil phase, ii) type and saturation of the surfactant, and iii) pos:neu lipid molar ratio of the surfactants (Table I).

Unsaturated squalene and saturated squalane were chosen as the oil phases. They are both isolated from animal or plant sources and are biocompatible and well-tolerated in humans (12,15). Squalene is more frequently used than squalane in emulsions for vaccine adjuvants (12). Important for the choice of oil is on one hand that squalene may be more readily metabolized due its role as a precursor in the cholesterol biosynthesis than squalane (16). One the other hand, squalane may confer enhanced chemical stability to the emulsion compared to squalene, as it is less prone to oxidation due to the absence of double bonds (12,17). The optimal volume ratio between the oil phase and the water phase, the concentration of the surfactants, and the composition of the different surfactant mixtures were determined in pilot studies (results not shown). The final compositions of the emulsions included in the experimental design are shown in Table I and II.

The emulsions were prepared by melting the surfactants with low hydrophilic-lipophilic balance (HLB) numbers (Span 60/80) and DDA, DODA, DSPE, DOPE and MMG in the oil phase, followed by addition of the water phase containing the surfactants with high HLB numbers (Tween 60/80) dissolved in Tris-buffer (10 mM, pH 7.4). The process parameters (number of passes and process pressure) were selected in pilot studies (Supplementary data fig. 2). In brief, a pre-emulsification step applying HSM was introduced prior to microfluidization of the emulsions to facilitate the emulsification process. Microfluidization was employed for emulsification to facilitate maximal reduction of the particle size. The colloidal stability of the emulsions was also enhanced, because emulsions prepared by using HSM showed a tendency to creaming already one day after preparation. The emulsions prepared using microfluidization did not show any creaming during storage at 4°C for two weeks, which was the duration of the *in vivo* study.

To evaluate both humoral and CMI responses induced by the emulsions *in vivo*, the recombinant, *Ct* fusion antigen CTH522 was used for immunization. CTH522 contains T-cell epitopes and B-cell epitopes covering the most prominent *Ct* serovars (13). CTH522 adjuvanted with CAF01 is currently being tested in humans (Clinical trial no. NCT02787109). It is therefore well-suited for the evaluation of both antibody as well as CMI responses.

Phase Diagram of Squalene-Based Mixtures

A phase diagram was constructed for the mixtures containing squalene with the saturated surfactants and DDA (Sat $S_{mix}1$) to investigate the phase behavior of the mixtures at different ratios (*w*/w) of Tris-buffer, squalene, and Sat $S_{mix}1$ (Fig. 1a). Pre-mixed squalene and Sat $S_{mix}1$ at different ratios were titrated with Tris-buffer. The resulting mixtures were analyzed morphologically by light microscopy and polarized light microscopy. As expected, high ratios of Sat S_{mix} and squalene resulted in w/o emulsions containing crystals, presumably composed of precipitated surfactant(s) (Fig. 1b). Increasing the ratio of Tris-buffer resulted in phase inversion to o/w emulsions, and the crystals were dissolved. As o/w emulsions are desirable as adjuvants, the emulsions for the optimization experiment were chosen within the o/w area of the phase diagram, containing 10% oil phase and 2% S_{mix} (*w*/*v*), which was confirmed by polarized light microscopy (results not shown).

Physicochemical Characterization of Emulsions

The emulsion droplets had *z*-averages between 125 and 230 nm and PDIs between 0.12 and 0.43 (Fig. 2a). The type of oil and surfactant had an impact on the droplet size and PDI, and emulsions containing squalene and the unsaturated surfactants had the smallest average droplet sizes (Fig. 2a). Cryo-TEM of emulsions based on squalene or squalane with either Sat $S_{mix}1$ or Unsat S_{mix} 4 (Fig. 2b) confirmed the presence of emulsion droplets. It cannot be fully excluded that other small structures were present, but in any case, they were impossible to distinguish from artifacts from the ice. The size of the emulsion droplets apparent from the images corresponded well with the *z*-average measured by DLS. Thus, for most emulsions, the majority of droplets were smaller than approx. 150 nm, while the emulsion based on squalane with Unsat Smix 4 had a larger average droplet size (Fig. 2b).

The zeta-potential was highly dependent on the pos:neu lipid molar ratio, as a pos:neu lipid molar ratio of 2:0 resulted in a positive zeta-potential of the droplets (40–60 mV, Fig. 2c), comparable to the zeta-potential of CAF04, which is 40 mV (results not shown), as previously reported (7). At a pos:neu lipid molar ratio of 1:1, the cationic zeta-potential was slightly reduced (Fig. 2c). Interestingly, the emulsions with a pos:neu lipid molar ratio of 0:2 had negative zeta-potentials at the applied experimental conditions. As expected, the pos:neu molar lipid ratio had an influence on the zeta-potential (Fig. 2c). However, the choice of surfactant mix also affected the zeta-potential.

Rheological stress testing was performed to assess the mechanical strength of the emulsion system. When applying a shear stress to the emulsions (Fig. 2d), a significant decrease in the elastic modulus (G') was observed at oscillatory stress values of 0.15–0.25 Pa for the emulsions based on the Sat $S_{mix}1$. In contrast, measurements of emulsions based on the Unsat $S_{mix}4$ failed to establish a steady state, indicating that the emulsion systems were disintegrating even at minimal shear. The amount of stress needed to induce a significant

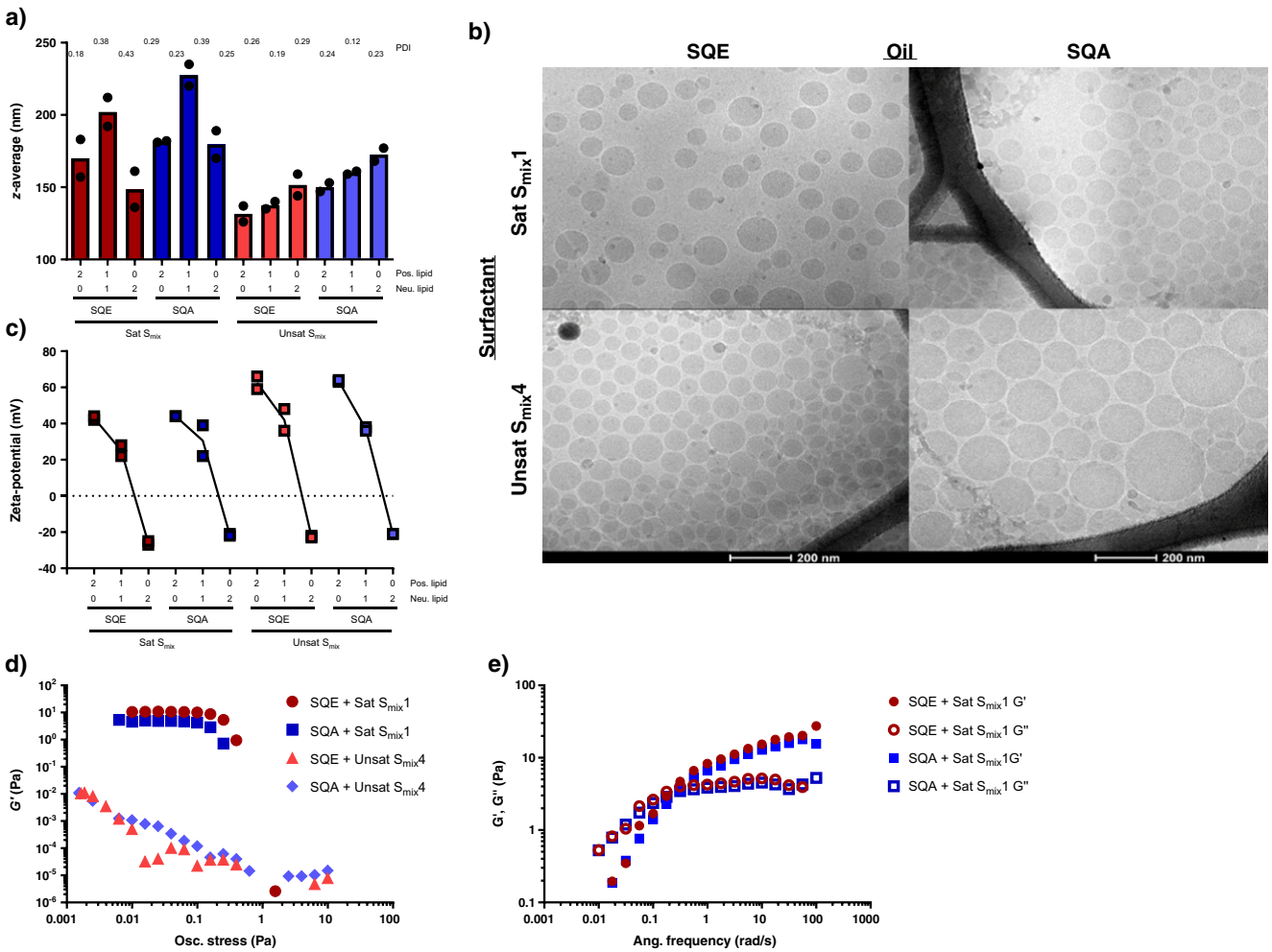

Fig. 2 Physicochemical characterization of emulsions prepared in the optimization experiment. (**a**) Hydrodynamic diameter. The columns represent the average of two different batches, while the dots represent the values of the individual batches. The numbers above the columns represent the average PDI values. (**b**) Representative cryo-TEM images of emulsions based on squalene or squalane combined with Sat S_{mix}1 or Unsat S_{mix}4. (**c**) The zeta-potentials of the emulsions. The dots represent the values of the individual batches. (**d**) Rheological stress measured on emulsions based on squalene or squalane combined with Sat S_{mix}1 or Unsat S_{mix}4. (**e**) Shear storage, G', and loss, G'', moduli dependent on applied frequency for emulsions based on squalene or squalane with Sat S_{mix}1. Data points represent one sample of duplicate measurements. SQE: squalene, SQA: squalane, pos. And neu. Lipid: ratio of positively charged lipids (DDA or DODA) or zwitterionic lipids (DSPE or DOPE) in the S_{mix}.

decrease in G', e.g., the force needed to disrupt the secondary bonds within the emulsion is likely to influence behavior, hence stability and performance during immunization. Thus, emulsions based on Sat S_{mix}1 are more likely to retain system integrity, whereas the emulsions based on Unsat S_{mix}4 might disintegrate during administration due to the shear stress introduced in the syringe upon administration. In addition, there might be differences in the kinetics of drainage and interaction with antigen-presenting cells, depending of the type of S_{mix}.

Moreover, dynamic frequency sweeps were performed for the emulsions based on squalene or squalane emulsified with S_{mix}1 (Fig. 2e). At frequencies below 0.2–0.3 rad/s, the shear storage modulus was lower than the shear loss modulus ($G' < G''$), indicating the that emulsions might behave as viscoelastic liquids (18). However, at higher frequencies the emulsions adopted what might be a gel-like structure with $G'' < G'$. Similar trends for G' and G'' were observed for the two emulsions at increasing frequencies, indicating the Sat S_{mix}1 is decisive for the behavior of the emulsions, whereas the type of oil (squalene or squalane) has no influence.

Emulsions with a Positive Zeta-Potential Combined with an Unsaturated Surfactant Induce CD4$^+$ T-Cell Responses

The adjuvants were evaluated for their ability to induce antibody and Th1/Th17 responses, because CAF04 has previously been reported to stimulate a mixed Th1/Th17 response (7). The CD4$^+$ T-cell responses were evaluated by quantifying the antigen-specific secretion of IFN-γ from isolated splenocytes restimulated with CTH522 measured by ELISA (Fig. 3a). In

addition, it was evaluated by counting the frequency of antigen-specific IFN-γ- and TNF-α-producing $CD4^+$ T cells in the spleen analyzed by intracellular staining and flow cytometry (Fig. 3b-c, for clarity only the emulsions with pos:neu lipid molar ratio of 2:0 are shown). Only vaccination with emulsions with a positive zeta-potential resulted in the induction of antigen-specific production of IFN-γ by restimulated splenocytes and increased frequencies of IFN-γ- and TNF-α-producing $CD4^+$ T-cells (Fig. 3a-c). Interestingly, of the emulsions with positive zeta-potentials, those containing Unsat $S_{mix}4$ and squalene induced significantly higher $CD4^+$ T-cell responses, as compared to the emulsions containing the Sat $S_{mix}1$ (Fig. 3). Accordingly, data analysis showed that the pos:neu lipid molar ratio and the choice of surfactant had a significant impact on the induced immune responses, whereas no significant effect was observed with regards to the choice of oil phase (Fig. 3). The rational choice of oil phase should thus be based on other factors, e.g., cost, biocompatibility, physical and chemical stability, prior clinical experience and availability.

The emulsion composed of squalene and Unsat $S_{mix}4$ containing DODA induced the strongest antigen-specific $CD4^+$ T-cell response, and the magnitude of the IFN-γ response was similar to the magnitude of the responses measured after vaccination with CAF04 (Fig. 3). Interestingly, the emulsions with a pos:neu lipid molar ratio of 1:1, which also had a positive zeta-potential, did not induce any antigen-specific $CD4^+$ T-cell responses. This may suggest that antigen adsorption takes place via attractive electrostatic interactions between the cationic emulsion droplets and the net negatively charged CTH522 protein (calculated theoretical isoelectric point value of 4.97, unpublished data), which results in emulsions with a neutral zeta-potential after adsorption of CTH522. This was confirmed by zeta-potential measurements (results not shown). Net neutral vaccine formulations in general show reduced uptake in antigen-presenting cells, compared to positively charged formulations (19,20), which explains the lack of immune response. However, further studies are needed to investigate the mechanisms of antigen adsorption and the cellular uptake.

High concentrations of IFN-γ were secreted from restimulated splenocytes isolated from mice vaccinated with CAF04 (Fig. 3a), as previously reported (7). This correlates well with the high frequencies of IFN-γ- and TNF-α-producing antigen-specific $CD4^+$ T-cells measured in the spleen (Fig. 3b-c). Antigen-specific $CD4^+$ T cells can be classified into cells with a potential effector-like or a potential memory-like phenotype, depending on their expression of IFN-γ, IL-2 and TNF-α (21). Mice immunized with emulsions containing the Unsat $S_{mix}4$ showed predominantly triple-positive and IFN-γ^+TNF-α^+ double-positive $CD4^+$ T-cell populations (Fig. 3d), which are mainly categorized as potential effector T cells (21). These populations are also present after immunization with CAF04, which in addition induced potential memory-like IL2$^+$TNF-α^+ and TNF-α^+ populations (Fig. 3d).

Fig. 3 Antigen-specific T-cell production of cytokines. Groups of four mice were immunized s.c. twice with 5 μg CTH522 plus the indicated adjuvants. One week after the last immunization, splenocytes were restimulated with CTH522 and (**a**) the levels of INF-γ were measured by ELISA, or the percentage of (**b**) TNF-α and (**c**) INF-γ producing $CD44^{high}$ $CD4^+$ T cells were determined by flow cytometry. Data are means ± SEM, n.s.: the group is not statistically different from the group vaccinated with CAF04-adjuvanted CTH522. All other groups were significantly different from the group vaccinated with CAF04-adjuvanted CTH522 (for clarity, statistics is not included in the figure). (**d**) Charts representing the frequencies of IFN-γ, IL-2 and TNF-α single-, double- and triple-producing activated $CD4^+$ T-cells following stimulaton with CTH522. The charts have been scaled to reflect the relative magnitudes of the $CD4^+$ T-cells responses between the immunization groups. (**e**) IL-17 producing $CD44^{high}$ $CD4^+$ T cells of splenocytes stimulated with CTH522, as determined by flow cytometry. SQE: squalene, SQA: squalane. Data are representative for two independent studies.

In Contrast to CAF04, Emulsions do Not Stimulate Th17 Responses

The CAF04 adjuvant has been shown to induce strong Th17 responses (7), which may be highly relevant for vaccines that should stimulate mucosal immune responses (22,23). We confirmed that CAF04 stimulates Th17 responses, but very little IL-17a was produced in response to restimulation with the antigen of splenocytes from mice immunized with all types of emulsions (Fig. 3e). There was a tendency that the emulsion with the Sat $S_{mix}1$ and squalane induced Th17 responses, although the measured IL-17a concentration was not significantly different from the concentration measured for the negative control. This emulsion has the closest resemblance to CAF04 in terms of composition. These findings indicate that it is not only the molecular composition of the adjuvant, which is decisive for the induction of Th17 responses, but also the way the immunopotentiators are presented by the delivery system (24). Further studies are needed to identify the exact mechanisms of action for Th17-stimulating adjuvants.

Emulsions and CAF04 Stimulate Comparable IgG Responses

There was a tendency to stronger induction of antigen-specific IgG1 and IgG2c responses by the emulsion with a positive zeta-potential containing squalene and Unsat $S_{mix}4$, as compared to the other emulsions and CAF04, as observed from the antibody titer curves (Fig. 4a-b). The induction of IgG2c responses was reduced for the emulsions containing Sat $S_{mix}1$, while the difference between the emulsions was less pronounced for the IgG1 responses (Fig. 4a-b). However, evaluation of the end-point titers showed no statistical significant difference between the emulsions and CAF04, however, the

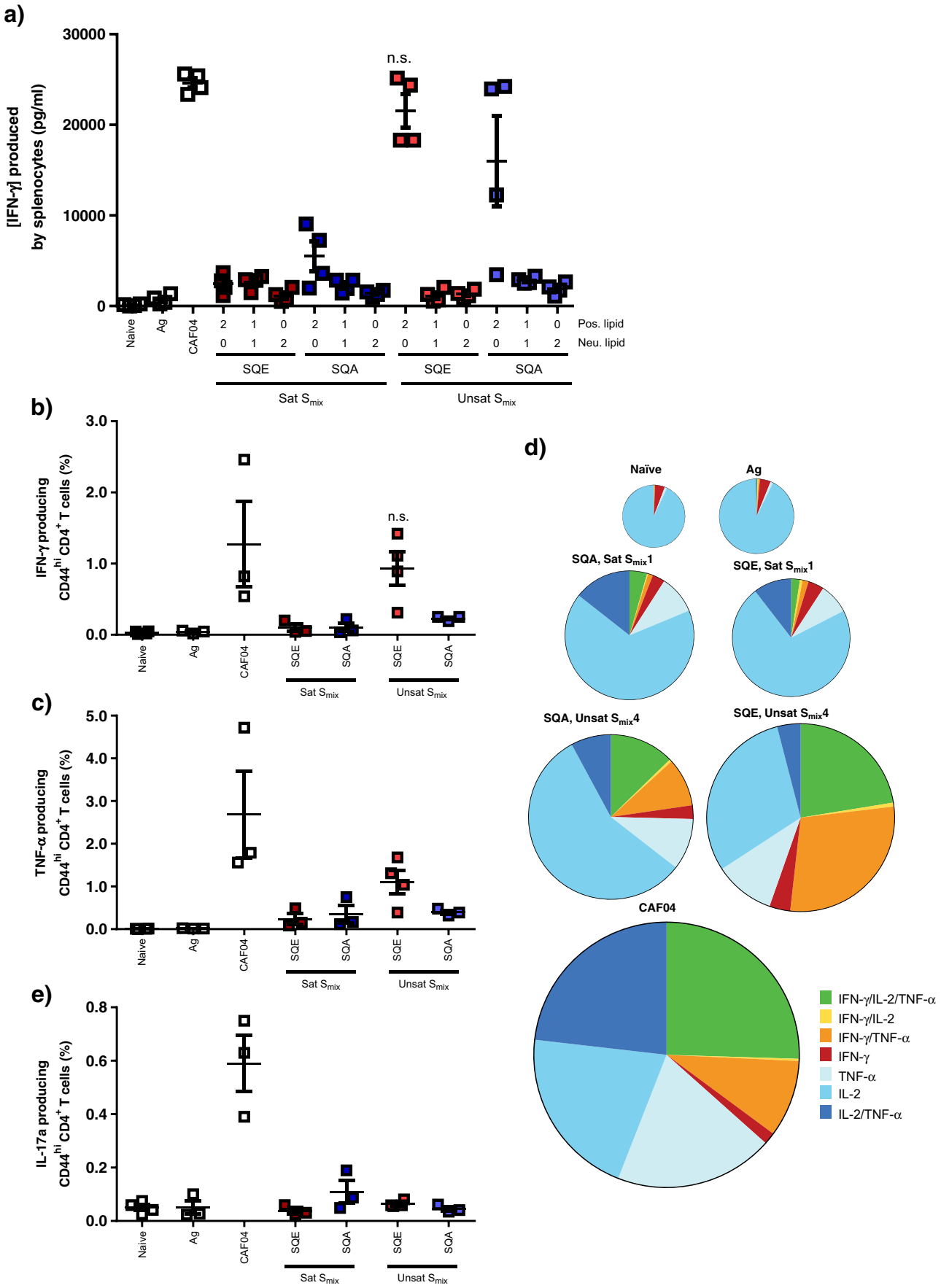
a)
[IFN-γ] produced by splenocytes (pg/ml)
30000
20000
10000
0
n.s.
Naive
Ag
CAF04
2 1 0 2 1 0 2 1 0 2 1 0 Pos. lipid
0 1 2 0 1 2 0 1 2 0 1 2 Neu. lipid
SQE SQA SQE SQA
Sat Smix
Unsat Smix
b)
IFN-γ producing CD44hi CD4+ T cells (%)
3.0
2.0
1.0
0.0
n.s.
Naive
Ag
CAF04
SQE
SQA
SQE
SQA
Sat Smix
Unsat Smix
c)
TNF-α producing CD44hi CD4+ T cells (%)
5.0
4.0
3.0
2.0
1.0
0.0
Naive
Ag
CAF04
SQE
SQA
SQE
SQA
Sat Smix
Unsat Smix
e)
IL-17a producing CD44hi CD4+ T cells (%)
0.8
0.6
0.4
0.2
0.0
Naive
Ag
CAF04
SQE
SQA
SQE
SQA
Sat Smix
Unsat Smix
d)
Naïve
Ag
SQA, Sat Smix1
SQE, Sat Smix1
SQA, Unsat Smix4
SQE, Unsat Smix4
CAF04
IFN-γ/IL-2/TNF-α
IFN-γ/IL-2
IFN-γ/TNF-α
IFN-γ
TNF-α
IL-2
IL-2/TNF-α

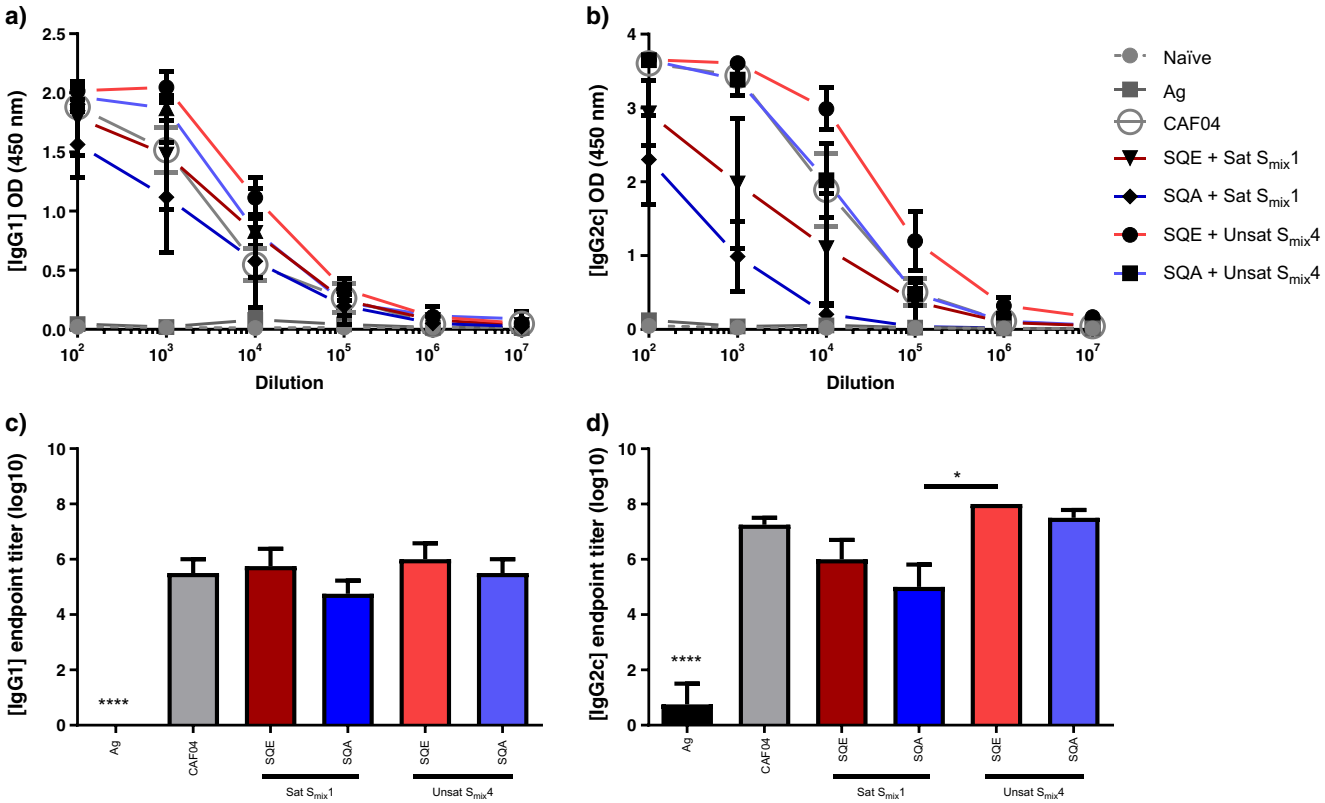

Fig. 4 Antigen (CTH522)-specific (**a**) IgG1 and (**b**) IgG2c levels in serum, and endpoint titers determined by ELISA of (**c**) IgG1 and (**d**) IgG2c. Groups of four C57BL/6 mice were immunized s.c. two times, and blood was drawn two weeks after the last immunization. Data are mean values ± SEM. **** $p \leq 0.0001$ for antigen-immunized mice as compared to all other groups, * $p \leq 0.05$. Data are representative for two independent studies.

emulsion with squalene and Unsat $S_{mix}4$ induced significantly higher IgG2c responses as compared to the emulsions with squalane and Sat $S_{mix}1$ (Fig. 4c-d).

DISCUSSION

A net positive zeta-potential has been shown to be required for stimulation of $CD4^+$ T-cell responses (25). Therefore, the correlation between the zeta-potential and the type of immune response observed in the current studies was expected: A pos:neu lipid molar ratio of 2:0 was essential for induction of $CD4^+$ T-cell responses following immunization with the emulsions, whereas immunization with the emulsions with a pos:neu lipid molar ratio of 0:2 did not induce any Th1 responses. A similar dependency of the zeta-potential on the immunological responses was observed in a comparative study of cationic CAF01 and neutral DSPC/TDB-liposomes, showing that only cationic CAF01 induced $CD4^+$ T-cell responses (25).

Immunization with emulsions containing the Unsat $S_{mix}4$ resulted in induction of higher $CD4^+$ T-cell responses, as compared to the responses induced with emulsions containing Sat $S_{mix}1$. Therefore, the saturation of the applied surfactant mixture is of importance. A comparative study of the immune responses stimulated by CAF01-adjuvanted antigen and antigen mixed with an adjuvant, where DDA was replaced with the unsaturated DODA, showed that immunization with liquid-state liposomes containing DODA did not stimulate a T-cell response (26). For the cationic liposomes, an increased membrane bilayer rigidity correlated with an increased ability to form a depot at the SOI, as well as co-localization of antigen [the recombinant *Mycobacterium tuberculosis* (*Mtb*) fusion antigen Ag85B-ESAT-6] and adjuvant in DCs in the dLNs (26). Formation of a depot of the antigen + adjuvant at the SOI and the concomitant co-delivery of antigen + adjuvant to DCs have been shown to be important prerequisites for the induction of $CD4^+$ T-cell responses with liposomal adjuvants (26,27).

For the emulsion-based adjuvants, the mechanisms of antigen adsorption, depot formation at the SOI and the concomitant delivery of antigen + adjuvant to DCs might be different. The cationic surface charge probably contributes to enhancing the co-delivery of antigen and adjuvant to DCs and macrophages at the SOI, because of the strong antigen adsorption via attractive electrostatic interaction and enhanced cellular uptake (20,28). However, delivery to the dLNs might be influenced by the fluidity of the surfactants. The MF59 adjuvant, which is based on squalene, Tween 80 and Span 85 (8), does not form a depot at the SOI, but is rapidly transported to the

dLNs, although antigen-positive cells are observed at the SOI for days (29,30). The proposed rapid clearance of the emulsion-based adjuvants from the SOI might influence the quality of the antigen-specific $CD4^+$ T-cell response, which is mainly of a potential effector-like type. In contrast, the continuous release of vaccine from a depot formed at the SOI following CAF04 immunization may result in stimulation of a stronger memory response. For yet unknown reasons, the uptake of the emulsions by antigen-presenting cells might be enhanced when the surfactants are unsaturated, as compared to the saturated surfactants. Biodistribution studies are currently being performed to track the vaccine after administration.

In case of the nanoemulsions designed in the present study, it appears that the introduction of an immunostimulator into a delivery system may enhance the capability of the adjuvant system to induce concomitant CMI and humoral responses. Thus, the incorporation of MMG-1 into the nanoemulsions is proposed to be necessary for the induction of $CD4^+$ T-cell responses. This was also the case in a comparative study, where different types of adjuvants, which are either clinically approved or under clinical investigation, were compared head-to-head in mouse models with antigens against *Ct* (MOMP), *Mtb* (Ag85B-ESAT-6-Rv2660c), and influenza virus (HA) (31). CAF01 was used in that study, but Th1/Th17-dominated CMI responses were induced with all antigens, comparable to those induced by CAF04 (4,7). Immunization with antigens adjuvanted with MF59 and Alum resulted only in strong humoral responses, whereas adjuvants containing an immunostimulator (CAF01, IC31 and GLA-SE) induced strong $CD4^+$ T-cell responses (31). However, the $CD4^+$ T-cell responses are also dependent on the antigen; GLA-SE induced stronger $CD4^+$ T-cell responses when combined with Ag85B-ESAT-6-Rv2660c, as compared to MOMP and HA (31). Adjuvants containing an immunostimulator have also been shown to be more effective for inducing $CD4^+$ T-cell responses in clinical studies. An increase in the $CD4^+$ T-cell responses was reported for adults vaccinated with AS03-adjuvanted TIV (32). GLA-SE was used as adjuvant for a respiratory syncytial virus (RSV) fusion protein and tested clinically in a phase Ia trial (11). Both humoral and CMI responses were reported, which were significantly higher than the responses measured for the unadjuvanted RSV fusion protein (11).

The tendency of the emulsion based on squalene and Unsat $S_{mix}4$ to induce stronger antibody responses than CAF04 may be correlated to the induction of $CD4^+$ T-cell responses, which help driving the class switching of the antibodies (33). However, CAF04 induces strong $CD4^+$ T-cell responses, so other mechanisms might also play a role for the induction of humoral responses by emulsions. For example, MF59 has been shown to be transported to the LNs by neutrophils within 1 h of i.m. immunization, and unprocessed antigen was located in the medullary compartments of the LNs (30,34). Other types of emulsion-based adjuvants have been shown to induce high antibody responses as compared to the cationic, liposome-based adjuvants (31).

CONCLUSION

Here we report the systematic design of a nanoemulsion-based adjuvant capable of inducing concomitant humoral and CMI responses. Systematic evaluation of the independent variables i) oil phase, ii) saturation of the surfactants, and iii) lipids with positively charged or neutral headgroups was utilized to investigate the influence of these factors on the physicochemical characteristics and immunological responses. The combination of a positive zeta-potential and unsaturated S_{mix} in the emulsion droplets resulted in stimulation of concomitant CMI and humoral responses.

ACKNOWLEDGMENTS AND DISCLOSURES

The work was funded by University of Copenhagen (STS) and Statens Serum Institut. Additional funding was provided by Innovation Fund Denmark [GeniVac (069–2011-1) and Centre for Nano-vaccine (grant number 09–067052)] and the European Commission through the ADITEC consortium contract (FP7-HEALTH-2011.1.4–4-280,873). The funding sources had no involvement in the study design; in the collection, analysis and interpretation of the data; in the writing of the report; nor in the decision to submit the paper for publication. We wish to thank the staff of the adjuvant group at INFIMM, SSI, in particular Janne Rabech and Rune Fledelius Jensen. We are grateful to Petra Alexandra Priemel, Department of Pharmacy, University of Copenhagen for technical assistance with the polarized light microscopy, and The Core Facility for Integrated Microscopy, Faculty of Health and Medical Sciences, University of Copenhagen. Karen Smith Korsholm, Peter Andersen and Dennis Christensen are employed by Statens Serum Institut, a nonprofit government research facility, which holds patents on the cationic liposomal adjuvants (CAFs).

REFERENCES

1. Rappuoli R. Bridging the knowledge gaps in vaccine design. Nat Biotech. 2007;25(12):1361–6.
2. Poland GA, Whitaker JA, Poland CM, Ovsyannikova IG, Kennedy RB. Vaccinology in the third millennium: scientific and social challenges. Curr Opin Virol. 2016;17:116–25.
3. Zepp F. Principles of vaccine design — lessons from nature. Vaccine. 2010;28(Suppl. 3):C14–24.

4. Agger EM, Rosenkrands I, Hansen J, Brahimi K, Vandahl BS, Aagaard C, *et al.* Cationic liposomes formulated with synthetic mycobacterial cord factor (CAF01): a versatile adjuvant for vaccines with different immunological requirements. PLoS One. 2008;3(9): e3116.
5. Nordly P, Rose F, Christensen D, Nielsen HM, Andersen P, Agger EM, *et al.* Immunity by formulation design: induction of high $CD8^+$ T-cell responses by poly(I:C) incorporated into the CAF01 adjuvant via a double emulsion method. J Control Release. 2011;150(3): 307–17.
6. Korsholm KS, Hansen J, Karlsen K, Filskov J, Mikkelsen M, Lindenstrøm T, *et al.* Induction of $CD8^+$ T-cell responses against subunit antigens by the novel cationic liposomal CAF09 adjuvant. Vaccine. 2014;32(31):3927–35.
7. Nordly P, Korsholm KS, Pedersen EA, Khilji TS, Franzyk H, Jorgensen L, *et al.* Incorporation of a synthetic mycobacterial monomycoloyl glycerol analogue stabilizes dimethyldioctadecylammonium liposomes and potentiates their adjuvant effect in vivo. Eur J Pharm Biopharm. 2011;77(1):89–98.
8. Brito LA, Malyala P, O'Hagan DT. Vaccine adjuvant formulations: A pharmaceutical perspective. Semin Immunol. 2013;25(2): 130–45.
9. Jackson LA, Campbell JD, Frey SE, *et al.* Effect of varying doses of a monovalent H7N9 influenza vaccine with and without AS03 and MF59 adjuvants on immune response: a randomized clinical trial. JAMA. 2015;314(3):237–46.
10. Nolan T, Bravo L, Ceballos A, Mitha E, Gray G, Quiambao B, *et al.* Enhanced and persistent antibody response against homologous and heterologous strains elicited by a MF59®-adjuvanted influenza vaccine in infants and young children. Vaccine. 2014;32(46):6146–56.
11. Falloon J, Ji F, Curtis C, Bart S, Sheldon E, Krieger D, *et al.* A phase 1a, first-in-human, randomized study of a respiratory syncytial virus F protein vaccine with and without a toll-like receptor-4 agonist and stable emulsion adjuvant. Vaccine. 2016;34(25):2847–54.
12. Fox C. Squalene emulsions for parenteral vaccine and drug delivery. Molecules. 2009;14(9):3286.
13. Olsen AW, Follmann F, Erneholm K, Rosenkrands I, Andersen P. Protection against Chlamydia trachomatis infection and upper genital tract pathological changes by vaccine-promoted neutralizing antibodies directed to the VD4 of the major outer membrane protein. J Infect Dis. 2015;212(6):978–89.
14. Frey A, Di Canzio J, Zurakowski D. A statistically defined endpoint titer determination method for immunoassays. J Immunol Methods. 1998;221(1–2):35–41.
15. Allison AC. Squalene and squalane emulsions as adjuvants. Methods. 1999;19(1):87–93.
16. Yarkoni E, Rapp HJ. Influence of type of oil and surfactant concentration on the efficacy of emulsified Mycobacterium Bovis BCG cell walls to induce tumor regression in guinea pigs. Infect Immun. 1980;28(3):881–6.
17. Romera SA, Hilgers LAT, Puntel M, Zamorano PI, Alcon VL, Dus Santos MJ, *et al.* Adjuvant effects of sulfolipo-cyclodextrin in a squalane-in-water and water-in-mineral oil emulsions for BHV-1 vaccines in cattle. Vaccine. 2000;19(1):132–41.
18. Valdez MA, Acedo-Carrillo JI, Rosas-Durazo A, Lizardi J, Rinaudo M, Goycoolea FM. Small-deformation rheology of mesquite gum stabilized oil in water emulsions. Carbohydr Polym. 2006;64(2):205–11.
19. Miller CR, Bondurant B, McLean SD, McGovern KA, O'Brien DF. Liposome−cell interactions in vitro: effect of liposome surface charge on the binding and endocytosis of conventional and sterically stabilized liposomes. Biochemistry. 1998;37(37):12875–83.
20. Foged C, Arigita C, Sundblad A, Jiskoot W, Storm G, Frokjaer S. Interaction of dendritic cells with antigen-containing liposomes: effect of bilayer composition. Vaccine. 2004;22(15–16):1903–13.
21. Seder RA, Darrah PA, Roederer M. T-cell quality in memory and protection: implications for vaccine design. Nat Rev Immunol. 2008;8(4):247–58.
22. Christensen D, Mortensen R, Rosenkrands I, Dietrich J, Andersen P. Vaccine-induced Th17 cells are established as resident memory cells in the lung and promote local IgA responses. Mucosal Immunol. 2016;10:260–70.
23. Lorenzen E, Follmann F, Bøje S, Erneholm K, Olsen AW, Agerholm JS, *et al.* Intramuscular priming and intranasal boosting induce strong genital immunity through secretory IgA in minipigs infected with Chlamydia trachomatis. Front Immunol. 2015;6:628.
24. Martin-Bertelsen B, Korsholm KS, Roces CB, Nielsen MH, Christensen D, Franzyk H, *et al.* Nano-self-assemblies based on synthetic analogues of mycobacterial monomycoloyl glycerol and DDA: supramolecular structure and adjuvant efficacy. Mol Pharm. 2016;13(8):2771–81.
25. Henriksen-Lacey M, Christensen D, Bramwell VW, Lindenstrøm T, Agger EM, Andersen P, *et al.* Liposomal cationic charge and antigen adsorption are important properties for the efficient deposition of antigen at the injection site and ability of the vaccine to induce a CMI response. J Control Release. 2010;145(2):102–8.
26. Christensen D, Henriksen-Lacey M, Kamath AT, Lindenstrøm T, Korsholm KS, Christensen JP, *et al.* A cationic vaccine adjuvant based on a saturated quaternary ammonium lipid have different in vivo distribution kinetics and display a distinct CD4 T cell-inducing capacity compared to its unsaturated analog. J Control Release. 2012;160(3):468–76.
27. Kamath AT, Mastelic B, Christensen D, Rochat A-F, Agger EM, Pinschewer DD, *et al.* Synchronization of dendritic cell activation and antigen exposure is required for the induction of Th1/Th17 responses. J Immunol. 2012;188(10):4828–37.
28. Korsholm KS, Agger EM, Foged C, Christensen D, Dietrich J, Andersen CS, *et al.* The adjuvant mechanism of cationic dimethyldioctadecylammonium liposomes. Immunology. 2007;121(2):216–26.
29. O'Hagan DT, Ott GS, De Gregorio E, Seubert A. The mechanism of action of MF59 – an innately attractive adjuvant formulation. Vaccine. 2012;30(29):4341–8.
30. Calabro S, Tortoli M, Baudner BC, Pacitto A, Cortese M, O'Hagan DT, *et al.* Vaccine adjuvants alum and MF59 induce rapid recruitment of neutrophils and monocytes that participate in antigen transport to draining lymph nodes. Vaccine. 2011;29(9):1812–23.
31. Knudsen NPH, Olsen A, Buonsanti C, Follmann F, Zhang Y, Coler RN, *et al.* Different human vaccine adjuvants promote distinct antigen-independent immunological signatures tailored to different pathogens. Sci Rep. 2016;6:19570.
32. Couch RB, Bayas JM, Caso C, Mbawuike IN, López CN, Claeys C, *et al.* Superior antigen-specific CD4(+) T-cell response with AS03-adjuvantation of a trivalent influenza vaccine in a randomised trial of adults aged 65 and older. BMC Infect Dis. 2014;14:425.
33. Moser M, Leo O. Key concepts in immunology. Vaccine. 2010;28(Suppl. 3):C2–C13.
34. Cantisani R, Pezzicoli A, Cioncada R, Malzone C, De Gregorio E, D'Oro U, *et al.* Vaccine adjuvant MF59 promotes retention of unprocessed antigen in lymph node macrophage compartments and follicular dendritic cells. J Immunol. 2015;194(4):1717–25.